PION-NUCLEON INTERACTION IN FREE SPACE AND ITS MEDIUM MODIFICATIONS*

C. SCHÜTZ, J.W. DURSO[1], K. HOLINDE, M.B. JOHNSON[2],

B.C. PEARCE[3] AND J. SPETH

Institut für Kernphysik, Forschungszentrum Jülich GmbH,
52425 Jülich,Germany

(Received July 7, 1993)

We report on a meson exchange model of the pion-nucleon interaction which has recently been developed by our group. Our model accounts for the πN phase shifts in the whole elastic region of the interaction, the low energy parameters and — by an extrapolation of the model to the Cheng–Dashen point — also the πN Σ term. Starting from a recent model of medium modifications of the $\pi\pi$ scattering amplitude we also investigate medium modifications of correlated 2π–exchange in the πN interaction. These modifications give rise to a considerable source of repulsion in the isoscalar S–wave pion optical potential and thus tend to resolve a longstanding puzzle.

PACS numbers: 25.80. Dj

1. Basic features of the πN interaction model

Recently, our group has developed a meson exchange model of pion–nucleon interaction [1]. It consists of two parts. First, there are direct and exchange nucleon and delta pole diagrams ((a) ... (d) in Fig. 1). The

---

* Presented at the Meson–Nucleus Interactions Conference, Cracow, Poland, May 14–19, 1993.

1 Present address: Dept. of Physics, Mount Holyoke College, MA 01075-1461, USA

2 Present address: Los Alamos National Laboratory, Los Alamos, New Mexico 87545, USA

3 Present address: Dept. of Physics and Math. Physics, Univ. of Adelaide, GPO Box 498, Adelaide, S.A. 5001, Australia

second part of the interaction model is given by potentials for the correlated exchange of two pions in the $0^{(+)}$ ('σ') and $1^{(-)}$ (ρ) channels ((e) in Fig. 1). These 2π–exchange processes have been approximated by sharp mass sigma and rho meson exchange in previous models of πN interaction [2, 3].

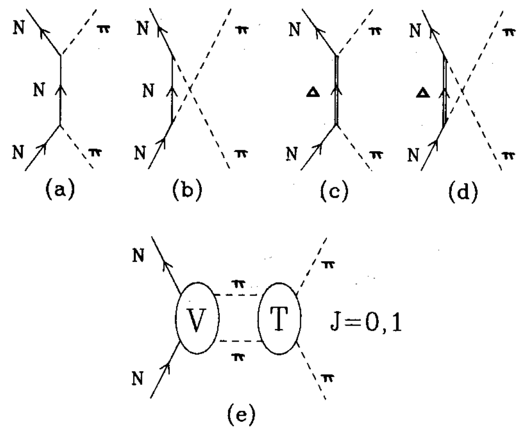

Fig. 1. Born term of the πN interaction model.

One essential advantage of our realistic treatment of correlated 2π–exchange is that we take explicitly into account the mass distribution of the exchanged 2π systems which, in our opinion, should not be neglected. Furthermore, our microscopic treatment of correlated 2π–exchange (see below) allows us to investigate the effect of medium–modifications of the πN interaction, which are not capable of being addressed in more conventional πN models.

Starting from our interaction model V the πN T-matrix is then obtained as the solution of a three-dimensional relativistic scattering equation of Lippmann–Schwinger type

$$T = V + VGT$$

within the framework of time-ordered perturbation theory.

2. The correlated 2π–exchange

The 2π–exchange part of the πN scattering amplitude kernel used in our work is constructed from $N\bar{N} \to \pi\pi$ partial wave helicity amplitudes $f_{\pm}^{J}$ [4] in the pseudophysical region ($t > 4\mu^2$), where J specifies the total angular momentum of the two exchanged pions. (In this paper μ denotes the pion mass and m the nucleon mass.) These amplitudes can be obtained from two sources. First, they have been determined in an analysis of experimental data of πN and $\pi\pi$ scattering [5]. Furthermore, we are able to calculate these amplitudes in a microscopic model. This model contains N– and Δ–exchange and ρ–pole Born diagrams and a $\pi\pi$ interaction model [6] which is likewise based on meson exchange. The predictions of our free space πN interaction model are of comparable quality for both choices of the input. For the calculations in this and the following chapter the pseudoempirical values of the $f^J_\pm$ amplitudes [5] have been used.

From the J=0 and J=1 helicity amplitudes one may construct the corresponding contributions to the pion–nucleon potential, which has the following general structure:

$$V^{(i)}_{\pi N} = C\,\bar{u}(p')[A_{(i)} + \not{Q} B_{(i)}]u(p)\,, \tag{1}$$

where $C = -m/(16\pi^3\sqrt{\omega_\pi \omega_{\pi'} E_N E_{N'}})$. Furthermore, $\not{Q} \equiv \gamma^\mu Q_\mu$ with $Q = {}^1\!/_2(q + q')$, where q and q' denote the four-momenta of the incoming and outgoing pion.

For the scalar ($i = \sigma$) and rho–meson ($i = \rho$) channels the amplitudes $A_{(i)}$ and $B_{(i)}$ are given by the dispersion integrals

$$A_\sigma = A^{(+)}_\sigma(t) = -(t - 2\mu^2) \int\limits_{4\mu^2}^{50\mu^2} \frac{4\,\mathrm{Im}\, f^0(t')dt'}{(\frac{1}{4}t' - m^2)(t' - t)(t' - 2\mu^2)}$$

$$B_\sigma = 0\,, \tag{2}$$

and

$$A_\rho = A^{(-)}_\rho(t, x)$$

$$= 12\frac{q_t}{p_t}x \left(\frac{m}{\sqrt{2}} \int\limits_{4\mu^2}^{50\mu^2} \frac{\mathrm{Im}\, f^1_-(t')}{t' - t} dt' - \int\limits_{4\mu^2}^{50\mu^2} \frac{\mathrm{Im}\, f^1_+(t')}{t' - t} dt' \right),$$

$$B_\rho = B^{(-)}_\rho(t) = \frac{12}{\sqrt{2}} \int\limits_{4\mu^2}^{50\mu^2} \frac{\mathrm{Im}\, f^1_-(t')}{t' - t} dt'\,, \tag{3}$$

where q_t and p_t are the momentum of the pion and the nucleon, respectively, in the t–channel, and x is the cosine of the scattering angle in this channel. $A^{(+)}$ and $A^{(-)}$ ($B^{(+)}$ and $B^{(-)}$) are the isospin even and odd invariant amplitudes forming A and B. For the σ channel only the isospin even part contributes and for the ρ channel only the isospin odd part.

In Eq. (2) a subtraction has been made in the dispersion relation at the Cheng–Dashen point ($t = 2\mu^2$). In combination with the pseudovector coupling used at the $NN\pi$ vertices (Fig. 1(a),(b)), this subtraction ensures that in Born approximation the scattering amplitude $T^{(+)} = A^{(+)} + \nu B^{(+)}$ vanishes at the Cheng–Dashen point (consistent with chiral symmetry). In fact, our result in Eq. (2) corresponds to a potential for scalar meson exchange in the πN system using derivative coupling at the $\pi\pi\sigma$ vertex, and it can easily be shown to give a *repulsive* contribution to the potential $V_{\pi N}^{(\sigma)}$ (in the S–waves).

According to the Cheng–Dashen theorem, the full amplitude at the Cheng–Dashen point is given by

$$T^{(+)}(\nu = 0, \nu_B = 0, q^2 = \mu^2, q'^2 = \mu^2) = \frac{\Sigma}{f_\pi^2}, \tag{4}$$

were f_π denotes the weak pion decay constant and Σ the πN Σ–Term. For our full model, which is discussed in the next chapter, we have performed an extrapolation below πN threshold to the Cheng–Dashen point. Using Eq. (4) our model yields as the prediction for the πN Σ–term $\Sigma = 69\,\text{MeV}$, which is in good agreement with the empirical value $\Sigma = 64 \pm 8\,\text{MeV}$ [7].

It is interesting to compare the potential resulting from Eq. (2) with the potential for the exchange of a zero width ρ meson in the πN system. In this case the invariant amplitudes A and B are given by [7]

$$A^{(-)}(t,x) = -\frac{p_t q_t x}{m}\frac{G_{\rho\pi\pi}G^T_{NN\rho}}{m_\rho^2 - t}; \quad B^{(-)}(t,x) = \frac{G_{\rho\pi\pi}(G^V_{NN\rho} + G^T_{NN\rho})}{m_\rho^2 - t}. \tag{5}$$

$G^V_{NN\rho}$ and $G^T_{NN\rho}$ are the coupling constants for vector and tensor coupling at the $NN\rho$ vertex, $\kappa \equiv G^T_{NN\rho}/G^V_{NN\rho}$. These coupling constants have been determined from experimental data [7] to be $G_{\rho\pi\pi}G^V_{NN\rho}/4\pi = 2.4$, $\kappa = 6.6$ at the rho pole ($t = m_\rho^2$).

The resulting on–shell potentials are plotted in Fig. 2. Obviously the potentials for the $1^{(-)}$ correlation and zero width ρ exchange differ considerably, especially in the S_{11} partial wave, which is of crucial importance for the description of πN scattering data. This discrepancy can be understood if one realizes that the coupling constants have been determined *for* $t = m_\rho^2$ whereas t *is always negative in the kinematic range of* πN *scattering.*

By setting the amplitudes (5) equal to (3) one can define effective, t–dependent coupling constants which parametrize the correlated 2π–exchange in the $1^{(-)}$ channel in terms of sharp rho exchange. For $t = 0$, *i.e.* at the πN threshold, one then finds the values $(G_{\rho\pi\pi}G^V_{NN\rho})^{\text{eff}}/4\pi = 5.0$, $\kappa^{\text{eff}} = 2.7$.

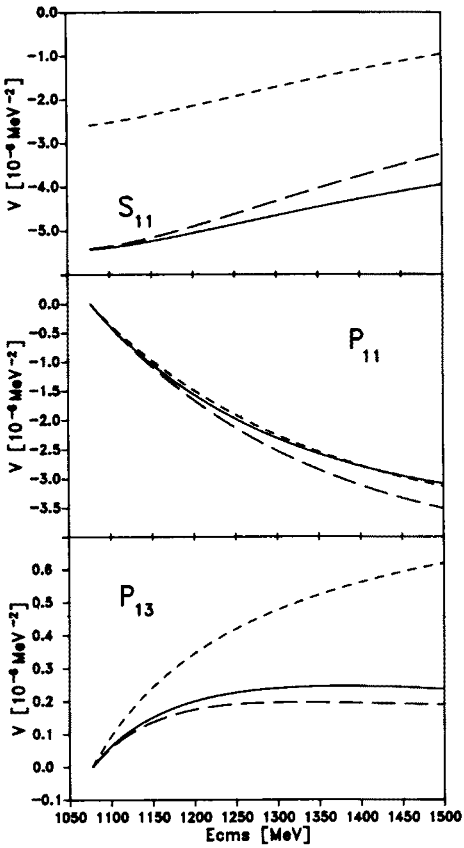

Fig. 2. On–shell potentials for rho exchange: The full line denotes the potential for correlated 2π–exchange in the $1^{(-)}$ channel, the short–dashed line represents zero width ρ–exchange using the parameters given in [7], the long–dashed line represents zero width ρ–exchange using effective parameters.

As can be seen from Fig. 2, with these effective coupling constants the potentials for correlated 2π –exchange and zero width ρ exchange agree much better.

In conclusion, if one wants to describe the $1^{(-)}$ correlation in πN interaction by a sharp ρ exchange, one needs much more vector and less tensor coupling compared to the coupling constants extracted at the rho pole. This result justifies the phenomenological findings of Ref. [2], where values for κ in the range from 1.4...3.2 have been used for the fit of πN scattering data.

3. Pion nucleon interaction in free space

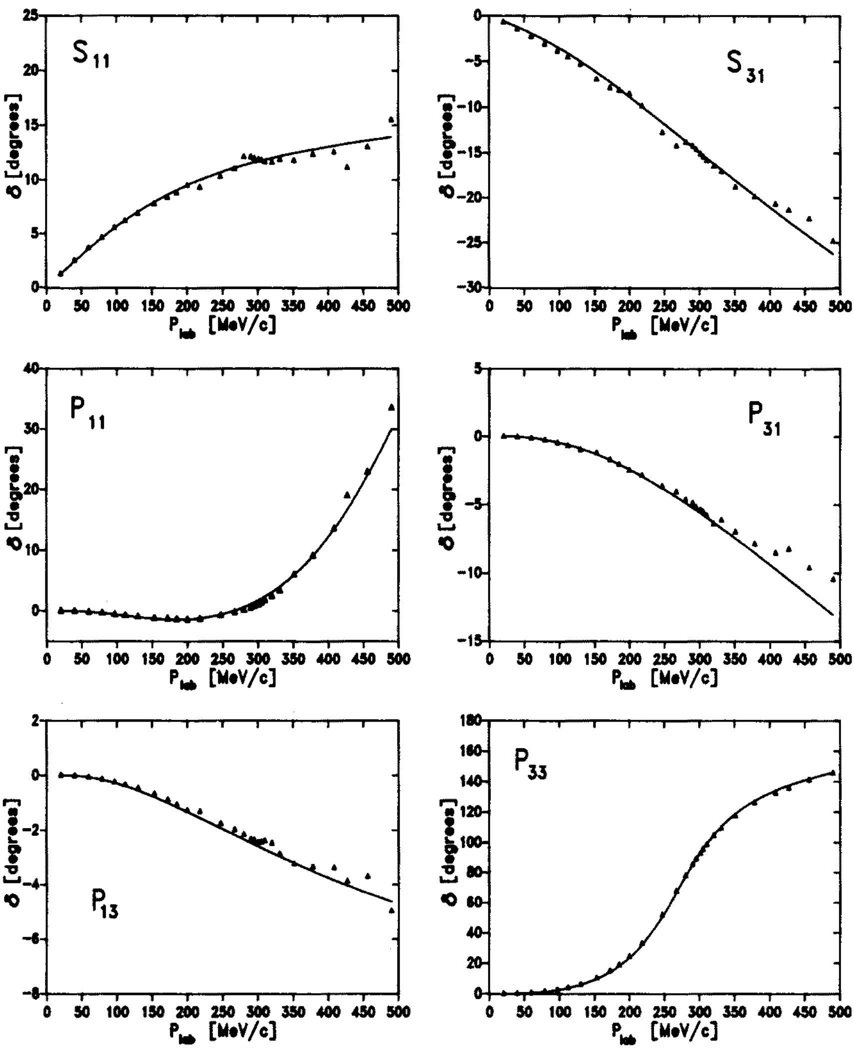

Fig. 3. S– and P–wave phase shifts obtained with our πN interaction model compared to the Karlsruhe phase shifts [9].

For this calculation coupling constants at the $NN\pi$ and $N\Delta\pi$ vertices have been taken from the Bonn NN model [8]. The same cannot be done for the formfactor parameters (cutoff masses) since, compared to NN scattering, we are now in a quite different kinematic region. Therefore the cutoff parameters for the contributions to the pseudopotential (Fig. 1) have been treated as free parameters to be adjusted to the πN scattering data. The bare Δ mass and the bare $N\Delta\pi$ coupling constant appearing in the Δ pole diagram (Fig. 1(d)) are adjusted to reproduce the P_{33} phase shift. The bare nucleon mass and the bare $NN\pi$ coupling constant for the nucleon pole contribution (Fig. 1(b)) are determined in a renormalization procedure as function of the other parameters. This renormalization ensures that our full T-matrix has a pole at the nucleon mass with the residue determined by the physical $NN\pi$ coupling constant.

Fig. 3 shows the resulting S- and P-wave phase shifts compared to the values of the Karlsruhe analysis [9].

The rise of the P_{11} phase shift is obtained without an explicit pole term for the N^*. The description of this partial wave is based on the cancellation between the strong attraction from correlated 2π-exchange and a repulsive contribution from the nucleon pole term. Though we do not need a contribution from a genuine N^* for the description of elastic πN scattering, it is necessary to extend the energy range of our model to higher energies to get a final answer to the question whether a contribution from a genuine N^* is needed to describe the P_{11} partial wave of πN scattering. Work in this direction is planned for the near future.

Furthermore, we have calculated the low energy parameters (scattering lengths and volumes) within this model to investigate to what extent our model is able to describe the threshold behaviour of πN scattering. The scattering lengths/volumes are defined by

$$a_L = \lim_{q\to 0} \frac{\sin 2\delta_L}{2q^{2L+1}}, \tag{6}$$

where q denotes the CMS momentum and L the orbital angular momentum. These low energy parameters compared to the empirical values given in Ref. [9] are listed in Table I. We find satisfactory agreement between our model and the empirical data.

TABLE I

The scattering lengths and volumes. Units are m_π^{-2L+1}.

	model	Koch *et al.* [9]
S_{11}	0.169	0.173 ± 0.003
S_{31}	−0.084	-0.101 ± 0.004
P_{11}	−0.083	-0.081 ± 0.002
P_{31}	−0.043	-0.045 ± 0.002
P_{13}	−0.031	-0.030 ± 0.002
P_{33}	0.210	0.214 ± 0.002

4. Medium Modifications of πN interaction

Our microscopic model of correlated 2π–exchange, which contains an explicit $\pi\pi$ scattering amplitude, enables us to calculate the modifications of the potentials for 'σ'– and ρ–exchange in the medium in a well–defined way [10].

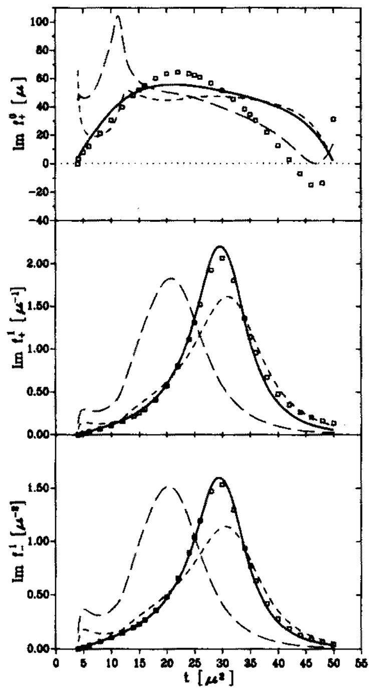

Fig. 4. The $N\bar{N} \rightarrow \pi\pi$ amplitudes in the pseudophysical region: The full line denotes our vacuum model, the short–dashed line represents medium modifications due to softening of the pion dispersion relation (for $\rho = \rho_0$) and the long–dashed line represents additional inclusion of the effect of dropping rho meson mass. The squares denote the values given in [5].

Medium modifications of the $\pi\pi$ scattering amplitude arise from the softening of the pion dispersion relation given by $\omega^2 = \mu^2 + k^2 + \Pi(k, \omega)$, where $\Pi(k, \omega)$ is the (density–dependent) pion self–energy [11]. This model of medium modifications can be extended to include changes of the chiral vacuum condensate $\langle 0|\bar{q}q|0\rangle$. As was shown in Ref. [12], these changes result in a linear decrease of vector meson masses with density (meaning that the ρ–meson mass appearing in the $\pi\pi$ pseudopotential is lowered by about $18\%\rho/\rho_0$). These medium modifications of the $\pi\pi$ scattering amplitude lead to modifications of the amplitudes Im $f^{0,1}_{(\pm)}$, which are the input for our calculation of correlated 2π–exchange (*cf.* Eqs (2), (3)).

The various medium modifications are shown in Fig. 4, for $\rho = \rho_0$, compared to the values of the vacuum f-amplitudes given by the Karlsruhe analysis [5]. The solid line denotes the result of our model for the vacuum f-amplitudes, which is in good agreement with the empirical data. In our first medium–modified model we only take into account the softening of the pion dispersion relation (short-dashed lines in Fig. 2). In addition, the effect of dropping rho mass is implemented in the second model (long-dashed lines in Fig. 2).

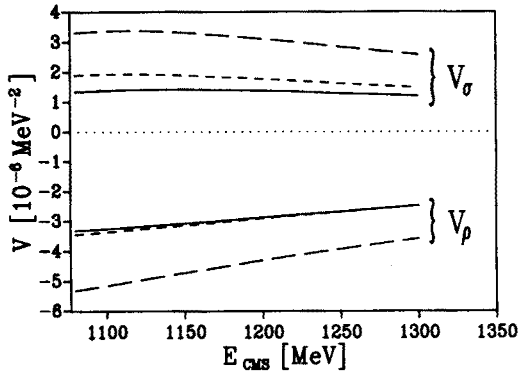

Fig. 5. Medium modifications of the S_{11}–wave potentials for correlated 2π–exchange in πN scattering (for $\rho = \rho_0$). The description of the curves is the same as in Fig. 4.

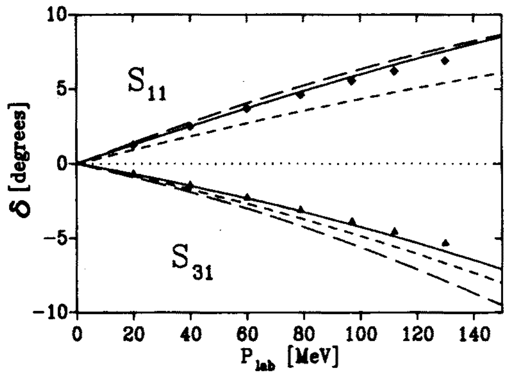

Fig. 6. Medium modifications of πN S–wave phase shifts due to modifications of correlated 2π–exchange (for $\rho = \rho_0$). The description of the curves is the same as in Fig. 4. Empirical data points are taken from [9].

After calculating the medium-modified πN potentials (1), which are plotted in Fig. 5, again for $\rho = \rho_0$, corresponding medium-modified πN phase shifts are obtained by iterating $V_{\pi N}$ in the scattering equation, *cf.* Fig. 6. Note that we have now adjusted the free parameters of the model to reproduce the empirical values of the S-wave scattering lengths [9] exactly for our vacuum calculation, because we want to discuss their modifications in the following.

As one can see from Figs 4–6, there are considerable effects, especially if the effect of dropping ρ-mass is implemented. If the ρ-mass is not dropped, $V_{(\rho)}$ remains essentially unchanged whereas the repulsion in $V_{(\sigma)}$ is increased due to the accumulation of strength near threshold in $\mathrm{Im}\, f_+^0$ (*cf.* Figs 4,5). The additional effect of dropping ρ-mass is drastic: There is an enormous downshift of strength in both $\mathrm{Im}\, f_+^0$ and $\mathrm{Im}\, f_\pm^1$ leading to a strong increase of the (repulsive) $V_{\pi N}^{(\sigma)}$ as well as the (attractive) $V_{\pi N}^{(\rho)}$.

5. The S-wave pion optical potential

The isoscalar S-wave pion-nucleus optical potential, $U_S^{(1)}$, is determined by the isoscalar S-wave scattering length b_0, $b_0 = {}^1\!/_3(2a_{31} + a_{11})$, through the relationship

$$U_S^{(1)} = -4\pi b_0 (1 + \frac{\omega_\pi}{m})\rho \,, \tag{7}$$

where ω_π is the relativistic laboratory energy of the pion and ρ is the sum of the neutron and proton densities. However, the Pauli correction is also important. In fact, it gives the major source of repulsion in the S-wave pionic atom potential. This term is often taken to be a correction of b_0, the net effect being called $\bar{b}_0$

$$\bar{b}_0 = b_0 - \frac{3k_F}{2\pi}(b_0^2 + 2b_1^2) \,, \tag{8}$$

with b_1 being the isovector S-wave scattering length, $b_1 = {}^1\!/_3(a_{31} - a_{11})$, and k_F the Fermi momentum. Using the empirical values of the πN scattering lengths [9] one finds $\bar{b}_0(\rho = \rho_0) = -0.035\,\mathrm{fm}$ and $\bar{b}_0(\rho = {}^1\!/_2\rho_0) = -0.032\,\mathrm{fm}$, respectively. On the other hand, from an analysis of pionic atom and low energy pion-nucleus scattering data [13] the empirical value of $\bar{b}_0$ turns out to be: $\bar{b}_0^{\mathrm{empirical}} = -0.046\,\mathrm{fm}$. So there is a considerable lack of repulsion in these results determined from Eq. (8) compared to the empirical value. The point now is that the medium-modifications discussed in the previous chapter change the scattering lengths and thus also $\bar{b}_0$. Without dropping the ρ-mass we find $\bar{b}_0(\rho = \rho_0) = -0.069\,\mathrm{fm}$ and $\bar{b}_0(\rho = {}^1\!/_2\rho_0) = -0.049\,\mathrm{fm}$, respectively. If we drop the ρ–mass in addition, we get $\bar{b}_0(\rho = \rho_0) = -0.059$ fm and $\bar{b}_0(\rho = {}^1\!/_2\rho_0) = -0.086$ fm, respectively.

Not surprisingly, the shift depends on the density as well as on the model used. Nevertheless, as a common feature, we have an even more repulsive $\bar{b}_0$ than the phenomenological analysis requires. A precise agreement should not have been expected however. First of all, additional modifications, *e.g.* in the meson–baryon form factors, cannot be ruled out. Second, the amount of dropping the ρ–mass is surely subject to a considerable uncertainty. It should be noted in this context that experiments to check the hypothesis of the dropping rho mass in the medium are in preparation [14]. In these experiments the dilepton decay of ρ mesons produced in relativistic heavy ion collisions will be investigated.

6. Summary

We have presented a meson–exchange model of the πN interaction. It consists, apart from conventional direct and exchange nucleon and delta pole diagrams, of correlated 2π–exchange processes, which replace the (to a large extent) fictitious sharp mass σ– and ρ–exchange contributions used before. The model provides a quantitative description of πN scattering data in the elastic region. Furthermore, it allows a well–defined investigation of medium effects. Corresponding modifications lead to an additional source of repulsion in the pion optical potential, apparently required for a precise understanding of pionic atom and pion–nucleus scattering data.

REFERENCES

[1] C. Schütz, Berichte des Forschungszentrums Jülich Nr. 2733, 1993; C. Schütz, J.W. Durso, K. Holinde, B.C. Pearce, J. Speth, in preparation.
[2] B.C. Pearce, B.K. Jennings, *Nucl. Phys.* **A528**, 655 (1991).
[3] P.F.A. Goudsmith, H.J. Leisi, E. Matsinos, *Phys. Lett.* **299B**, 6 (1993).
[4] W.R. Frazer, J.R. Fulco, *Phys. Rev.* **117**, 1603 (1960).
[5] G. Höhler, F. Kaiser, R. Koch, E. Pietarinen, *Handbook of Pion–Nucleon Scattering*, Physics Data 12-1, Fachinformationszentrum Karlsruhe 1979.
[6] D. Lohse, J.W. Durso, K. Holinde, J. Speth, *Nucl. Phys.* **A516**, 513(1990).
[7] G. Höhler, *Pion–Nucleon–Scattering*, Landolt–Börnstein Vol.I/9b2, ed. H. Schopper, Springer 1983.
[8] R. Machleidt, K. Holinde, Ch. Elster, *Phys. Rep.* **149**, 1 (1987).
[9] R. Koch, E. Pietarinen, *Nucl. Phys.* **A336**, 331 (1980).
[10] C. Schütz, K. Holinde, M.B. Johnson, J. Speth, to be published in *Phys. Lett.* **B**.
[11] V. Mull, J. Speth, J. Wambach, *Phys. Lett.* **286B**, 13 (1992).

[12] T. Hatsuda, S. H. Lee, *Phys. Rev.* **C46**, R34 (1992).
[13] J.A. Carr, H. McManus, K. Stricker–Bauer, *Phys. Rev.* **C25**, 952 (1982).
[14] V. Metag, private communication.